

## Electronic Supplementary Information

### Diffusion of hydrogen in graphite: A possible method for large-scale production of graphene

Ali Reza Kamali and Derek J. Fray

Department of Materials Science and Metallurgy, University of Cambridge, 27 Charles Babbage Road, Cambridge CB3 0FS

#### 1. X-ray diffraction characterization of the pristine graphite material

The X-ray diffraction pattern of the pristine graphite material in the  $2\theta$  range from  $20^\circ$  to  $40^\circ$  is exhibited in Fig. 1a. The prominent and sharp peak in the profile at  $2\theta = 26.441^\circ$  corresponds to the (002) peak of graphite with an interlayer distance of 0.337 nm. Table 1S summarises XRD data for the hexagonal (002) peak of the pristine graphite material.

Table 1S- XRD data for the hexagonal (002) peak of the pristine graphite material.

2-theta position (degrees)	26.441
Lattice spacing $d_{002}$ (nm)	0.337
Full width at half maximum (degrees)	0.246
Crystalline domain size $L_c$ (002) (nm)	33.2

#### 2. Cell potentials during the electrochemical process

The potential difference between both the graphite rod and the graphite crucible with reference to a Mo pseudo-reference electrode immersed in molten LiCl was measured during the electrochemical process, and the results are shown in Fig. 1S. According to Fig. 1S, the average cell potential during the process was about 8.7 V. However, as can be seen in Fig. 1, the electrodes were connected to the potential terminals by stainless steel rods of 3cm in diameter and 50 cm in length, causing a potential loss of about 4.7 V at the current of 33 A along two SS rods. With this in mind, the actual potential difference between the graphite

cathode and the graphite crucible can be assumed to be about 4 V in average, as shown in Fig. 1S.

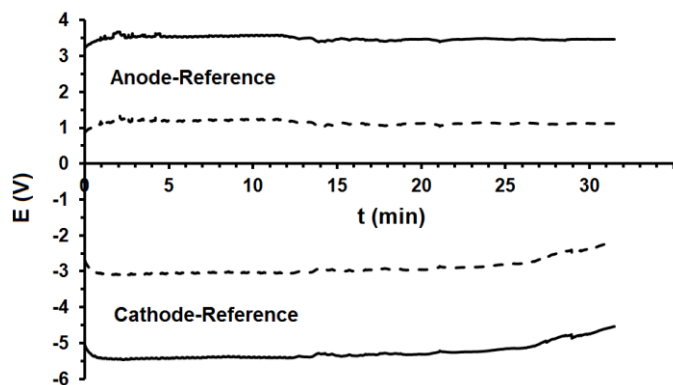
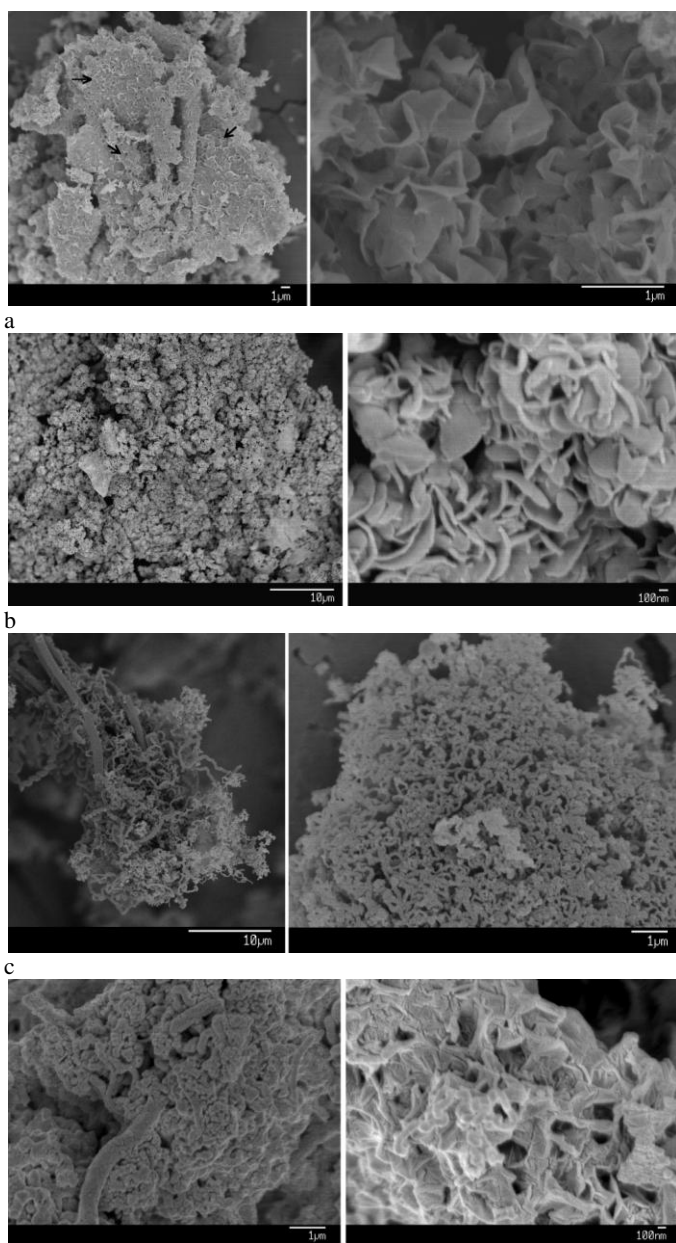


Fig. 1S. The apparent (solid lines) and actual (dotted lines) potential difference between both the graphite electrodes and a Mo pseudo-reference electrode immersed in molten LiCl. The electrodes were polarized in humid Ar atmosphere at a constant current of 33 A.

### 3. SEM characterization of the as-synthesized carbonaceous material

Fig. 2S shows the various morphologies observed in the as-synthesized carbonaceous material. The SEM sample was sputter-coated with a thin gold layer prior to the SEM examination. Fig. 2S-a, left, shows stacks of graphite sheets which are partially peeled off into segments. The arrows in the image point to some peeled area for instance. Fig.2S-a, right, demonstrates that the segments on graphite flakes are in fact nanosheets with sizes of several hundred nanometres. Fig. 2S-b, left, shows the dominant morphology observed in the sample, which is characterised by a completely exfoliated structure. The right panel in Fig.2S-b displays a higher magnification of the same region, demonstrating the formation of flower like nanosheets. The comparison of the Figs. 2S-a and b indicates that the carbon product may be formed by the progressive peeling off the graphite layers occurred during the molten salt process. Apart from the major morphology of nanosheets, several minor morphologies were also found in the material including carbon fibres (Fig. 2S-c) and irregular structures (Fig. 2S-d). The charging effect could be more observed on the irregular structures during operating the SEM, indicating the presence of non-conductive  $\text{Li}_2\text{CO}_3$  and LiCl.



d  
 Fig. 2S. SEM micrographs of various morphologies which could be observed in the as-synthesised carbonaceous material comprising of (a) partly and (b) fully exfoliated graphite sheets, (c) carbon fibres, and (d) irregular structures.

#### 4. Thermal analysis studies

DSC and TG analyses were performed on the pristine graphite feed material, the as-synthesised carbonaceous materials and the graphene nanosheets. The pristine graphite

material was ground into powder prior to thermal analyses. The experiments were conducted at a rate of  $40\text{ }^{\circ}\text{C min}^{-1}$  under ambient air of flow rate  $100\text{ mL min}^{-1}$ . Fig. 3S presents the curves recorded. The DSC thermogram of the pristine graphite powder exhibits an exothermic peak with the maximum at  $868\text{ }^{\circ}\text{C}$  which is due to the oxidation of graphite. From the corresponding TG analysis, the significant mass loss starts at about  $710\text{ }^{\circ}\text{C}$ . The DSC thermogram of the as-synthesised carbonaceous material shows two exothermic peaks at  $448$  and  $615\text{ }^{\circ}\text{C}$ . The first peak which corresponds to the most significant mass loss occurred (see the corresponding TG curve) can be attributed to the oxidation of nano-sized carbon constituents, and the second peak to the oxidation of the micrometer-sized carbon particles. The later are incompletely degraded pieces of graphite that become detached from the cathode during the electrolysis process. The low oxidation resistance of the as-synthesized carbonaceous material was found to be due to the presence of lithium carbonate nano-single crystals in the microstructure of the material, which are active catalysts for the carbon oxidation [1]. The DSC thermogram of the graphene nanosheets displays a single oxidation peak at  $515\text{ }^{\circ}\text{C}$ . The corresponding TG peak shows that the main mass loss starts at  $450\text{ }^{\circ}\text{C}$ . As depicted from Fig. 1c, the amount of  $\text{Li}_2\text{CO}_3$  in graphene nanosheets was below the detection limit of XRD resulting in a higher oxidation resistance of graphene nanosheets than that of the as-synthesised carbonaceous material. However, on the other hand, the oxidation of graphene nanosheets is characterized by a single exothermic peak which indicates the high degree of microstructural homogeneity of the material. Moreover, the high ratio of edge/basal planes in graphene makes the material susceptible to oxidation in comparison to the pristine graphite. This is because while the basal plane of graphite is very difficult to oxidize with molecular oxygen, the edges of basal plane are quite active due to the presence of free bonded atoms, and therefore oxidize more readily [2]. Although the graphene nanosheets

were oxidized at a lower temperature than the pristine graphite, yet are thermally stable below 450 °C which is due to their high degree of crystallinity.

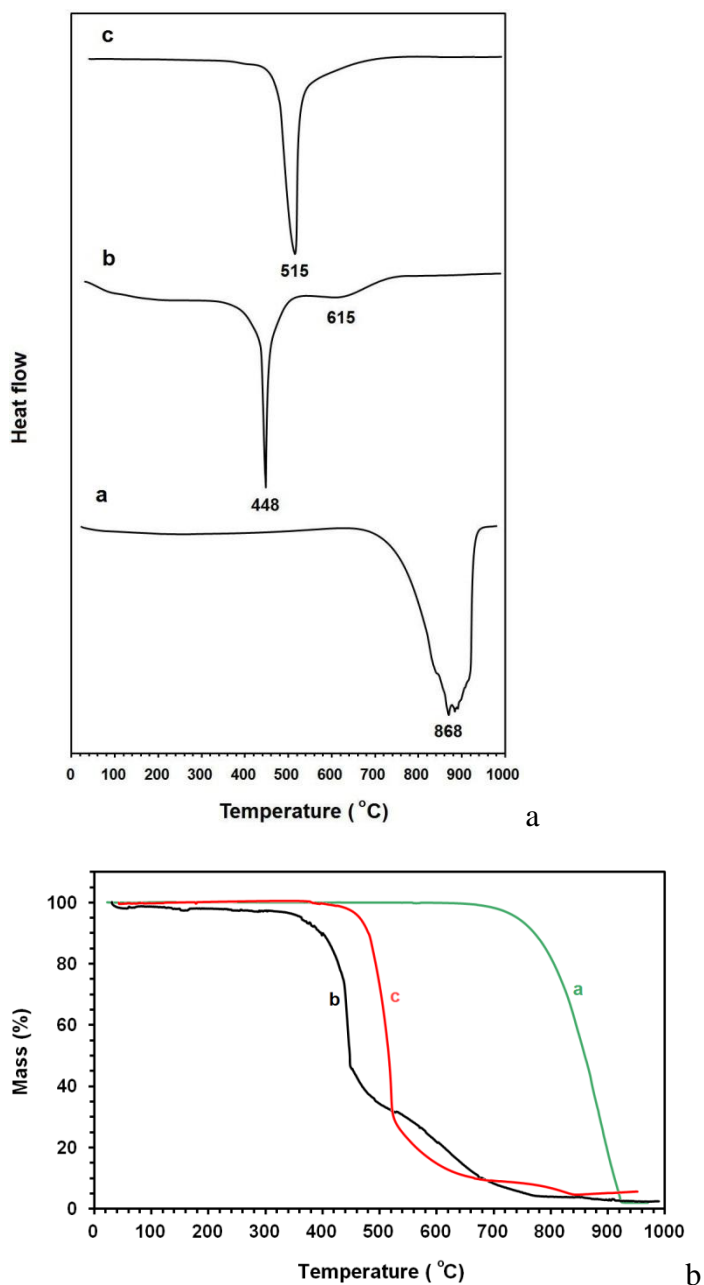


Fig. 3S. (Upper panel) DSC and (down panel) TG curves for (a) the pristine graphite powder, (b) as-synthesised carbonaceous material, and (c) graphene nanosheets heated at a rate of 40 °C min<sup>-1</sup> under an ambient air flow of 100 mL min<sup>-1</sup>. The curves are plotted such that a downward peak corresponds to an exothermic transition.

## References

- [1] D.W. McKee, D. Chatterji, The catalytic behavior of alkali metal carbonates and oxides in graphite oxidation reactions. *Carbon* 13 (1975) 381–390.
- [2] Luo XW, Robin JC, Yu SY. Effect of temperature on graphite oxidation behavior. *Nucl Eng Des* 227 (2004) 273–80.